

## A Numerical Procedure for Coupled Consolidation in Saturated Soils

J. M. Horta Rangel<sup>1\*</sup>, R. Galaviz Gonzalez<sup>1</sup>, E. Rojas Gonzalez<sup>1</sup>, L. Pérez Rea<sup>1</sup>,  
T. Lopez Lara<sup>1</sup> and J. B. Hernandez Zaragoza<sup>1</sup>

<sup>1</sup>Department of Graduate Engineering, Universidad Autónoma de Querétaro, Cerro de las Campanas s/n, Querétaro, Qro. C.P. 76010, Mexico.

### Authors' contributions

This work was carried out in collaboration between all authors. Authors JMHR, RGG and ERG designed the study, performed the statistical analysis, wrote the protocol, wrote the first draft of the manuscript and managed literature searches. Authors LPR, TLL and JBHZ managed the analyses of the study and literature searches. All authors read and approved the final manuscript.

### Article Information

DOI: 10.9734/BJAST/2016/30219

#### Editor(s):

(1) Xu Jianhua, Department of Geography, East China Normal University, China.

#### Reviewers:

(1) Wenbing Wu, China University of Geosciences, China.

(2) Anonymous, Blaise Pascal University, France.

(3) Ujwalkumar Patil, University of Texas at Arlington, USA.

Complete Peer review History: <http://www.sciencedomain.org/review-history/17112>

Original Research Article

Received 25<sup>th</sup> October 2016  
Accepted 30<sup>th</sup> November 2016  
Published 3<sup>rd</sup> December 2016

### ABSTRACT

Consolidation is the reduction of soil volume with time. This phenomenon generates a stresses transfer process beginning with the application of load and subsequent increase in pore water pressure. This increase in pore water pressure generates a flow of water that reduces the volume of soil. Thus, consolidation represents a hydro-mechanical coupled problem. Different models have been developed to simulate this phenomenon properly. This paper presents a coupled hydro-mechanical consolidation model for saturated materials. It can also be extended to the case of unsaturated materials when effective stresses are used. This model considers different drainage, displacement and loading conditions. It properly simulates the phenomenon of consolidation and is consistent with other models. It also correctly reproduces laboratory tests.

**Keywords:** Coupled model; consolidation theory; saturated soil; dynamic solution; fluid-solid fields.

\*Corresponding author: E-mail: [jaimhorta@prodigy.net.mx](mailto:jaimhorta@prodigy.net.mx), [horta@uaq.mx](mailto:horta@uaq.mx);

## 1. BACKGROUND

A saturated porous medium, such as soils, can be considered as a deformable solid skeleton with all pores filled with fluid [1]. There are many geotechnical problems related to the consolidation of saturated soils. A very common one refers to the settlements of a foundation slab placed on the surface of a saturated material. The soil suffers volume decrease induced by the applied load. These volume changes may result in differential settlements producing the cracking of foundations [2,3]. It has been established that these damages are more expensive than those associated to natural disasters [4]. Additionally, volume changes are induced by the increase in pore water pressure generating a flow of water. This process is called consolidation [5]. The consolidation process involves the flow of water, the change in effective stresses and a volumetric reduction, hence it is considered as a coupled hydro-mechanical problem [6]. Unsaturated soils may reach the saturated condition when heavy rains occur or water pipe leaks [5,7].

Some coupled models have been developed to simulate the saturated consolidation, such as: Magaña and Romo [5], Bentler [7], Manzoillo et al. [8], Di-Rado et al. [9] and Krishnamoorthy [10]. These models are based on the following hypothesis: a) the soil is saturated, b) the solid and water phases are incompressible c) Darcy's law governs the behavior of flow through the soil. In addition, other authors have made improvements by incorporating different theories as for example: the theory of small deformations used by Bentler [6]. The principle of virtual work used by Manzoillo et al. [8] and the principle of mass conservation used by Manzoillo et al. [8] and Di-Rado et al. [9]. These latter employed the Terzaghi's effective stress and the Galerkin's solution method of weighted residuals, respectively. Besides, Krishnamoorthy [10] took into account the nonlinear behavior of soil and used the hyperbolic relationship of Duncan and Chang (1970). These models show consistent results with experimental tests. All these models have their advantages and disadvantages. However, the last model can be improved by combining some of the theories previously mentioned.

This has motivated the development of a new numerical procedure of coupled hydro-mechanical consolidation for saturated materials. This formulation considers the principles of the balance of momentum, the transient flow and

effective stresses where Terzaghi's principle is introduced. Initially, an inner product between the vector functions that takes into account the virtual work principle associated to the variational principle of the minimum potential energy is considered. In addition, the Finite Element Method (FEM) in combination with Galerkin's method that includes a time increment in which the evolution of displacements and pore water pressure are determined using an approximate solution.

As there are no analytical solutions for the hydro-mechanical coupling in unsaturated soils, numerical techniques, such as the Finite Element method needs to be used. This can be done when the mechanical consolidation equation, the soil-water retention curve (SWRC) and the permeability of the soil are combined [11]. Therefore, this procedure of coupled hydro-mechanical consolidation of saturated soils, can be extended to the unsaturated case. In such a case, the model uses Bishop's effective stress equation for unsaturated soils which includes the net stress  $(\sigma - u_a)$  and the matric stress  $\chi\psi$ , represented by the product of parameter  $\chi$  and soil suction. Both parameter  $\chi$  and the hydraulic conductivity can be obtained from the SWRC as a function of suction.

## 2. GOVERNING EQUATIONS

Due to seasonal changes, natural soils are subjected to cyclic wetting-drying cycles. When the water content is high, applied loads on the soil causes the flow of water and reduction of the soil volume. Thus, mechanical soil deformation and water flow represents a coupled field problem. Some assumptions include: a) the soil is fully saturated, b) the water and solid phase are incompressible, c) Darcy's law governs the flow of water. In addition, small deformations theory is used. So, according to the continuum mechanics theory the governing equations are as follow:

### i. Equilibrium Equations:

According to the Balance Law of Continuum Mechanics, and introducing the Piola-Kirchhoff Stress Tensor  $\underline{S}$  in Lagrangean Configuration; this tensor gives the force measured per unit area in the configuration of reference [12].

$$Div \underline{S} + \underline{b}_o = \ddot{\chi} \rho_o \quad (1)$$

Body forces commonly are considered as nil,  $\underline{b}_O = \underline{0}$ . Also acceleration field is considered nil,  $\ddot{\underline{x}} = \underline{0}$ , since the settlement process is considered as quasi-static.

ii. Continuity Equations

$$\text{div} \underline{v} - \dot{\underline{\varepsilon}} = 0 \quad (2)$$

where  $\underline{v}$  is the velocity field and  $\dot{\underline{\varepsilon}}$  is the derivative of the field strain.

iii. Darcy's Law

$$v_i = k_{ij} (\gamma_w h_i)_{,j} / \gamma \quad (3)$$

where  $k$  the coefficient of permeability of the soil,  $\gamma$  is the specific weight. Piezometric level  $h$  is evaluated according to the reference level  $z$ :  $h = p_w / \gamma_w + z$ .

iv. Boundary Conditions:

These conditions are related to the values of pore water pressure and stress at the boundaries. Also the surface inflow or outflow due to seasonal wetting-drying is considered. The total boundary  $\Omega$  conditions include both Dirichlet  $\Omega_D$  boundary and Newman's boundary  $\Omega_N$  conditions. Then, we can write these conditions in terms of the prescribed values:

a) Excess pore pressure conditions:

$$u = \hat{u} \quad \text{on} \quad \partial\Omega_D \quad (4)$$

b) Surface stresses:

$$\underline{S} \underline{n} = \hat{t} \quad \text{on} \quad \partial\Omega_N \quad (5)$$

c) Surface Inflow:

$$Q = \hat{Q} \quad \text{on} \quad \partial\Omega_i \quad (6)$$

Another condition is related to the inflow in the soil. This case can be observed as an induced water flow due to failure of sewers or water pipes.

d) Inflow inside the soil:

$$Q_s = \hat{Q}_s \quad \text{on} \quad \partial\Omega_i \quad (7)$$

### 3. CONSTITUTIVE EQUATION

The relationship between stresses and soil deformation follows the Hooke's Law. Stress Tensor  $\underline{S}$  involves stresses on the soil skeleton as on the pore water

$$\underline{S} = \underline{\bar{S}} + p_w \underline{I} \quad (8)$$

where:  $\underline{S}$  is the Tensor of stresses,  $p_w$  is the pore water pressure (considered as hydrostatic) and  $\underline{I}$  is the Identity Tensor  $= \sum_i e_i \otimes e_i$  (Tensor Nomenclature [12])

The procedure for establishing coupled equations is based on the virtual work principle. Discrete coupled equations are written as follows:

$$[K] \{U\} + [K_v]^T \{p\} = \{F\} \quad (9)$$

where  $[K]$  is the soil stiffness matrix,  $[K_v]^T$  is the transposed coupled matrix,  $\{U\}$  is the nodal displacements vector,  $\{p\}$  is the nodal water excess pore pressure,  $\{F\}$  is the external forces vector.

$$[K_v] \{\dot{U}\} + \frac{1}{\gamma_w} [K_h] \{p\} = \{Q\} \quad (10)$$

where  $[K_v]$  is the coupled matrix,  $[K_h]$  is the drained matrix,  $\{Q\}$  external/internal flow vector,  $\{\dot{U}\}$  velocity vector of nodal displacements.

Resulting matrices involve the following integral forms:

$$\begin{aligned} [K] &= \int_V [B_\phi]^T [\bar{D}] [B_u] dV \\ [K_v]^T &= \int_V [B_\phi]^T \langle 1 \ 1 \ 0 \rangle^T [N_p] dV \\ [K_h] &= \int_V [B_\theta]^T [k] [B_p] dV \end{aligned} \quad (11)$$

Matrices  $[B_i]$  contain derivatives of the shape function;  $[k]$  is the permeability matrix, and the vector  $\langle 1 \ 0 \ 0 \rangle^T$  is required to couple the degree of freedom of the two involved fields.

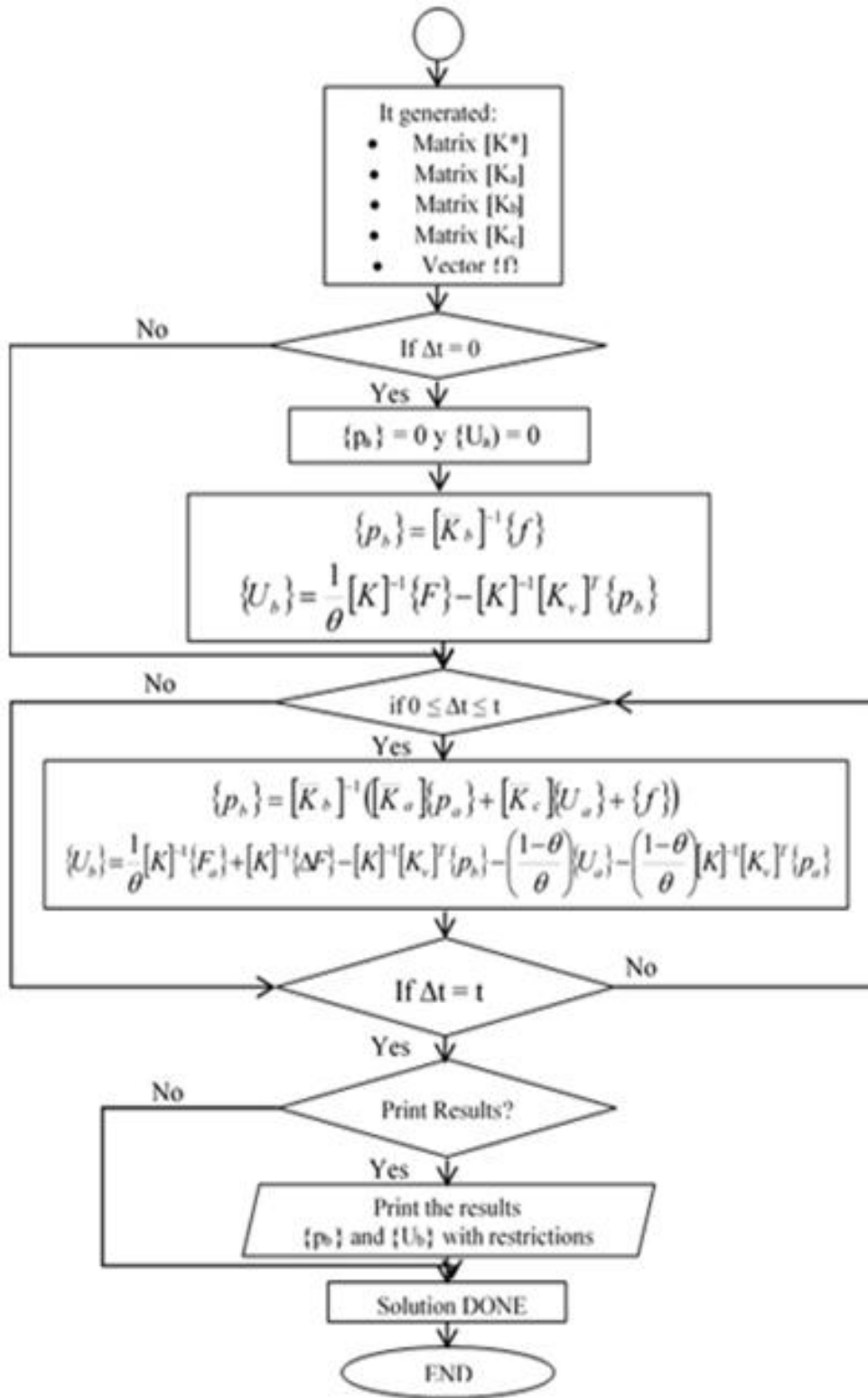


Fig. 1. Flowchart of the dynamic process of saturated consolidation coupled model

The resulting matrix equation associates the coupled hydro-mechanical consolidation model of saturated soils. Equations (9) and (10) can be written as a coupled equation:

$$\begin{bmatrix} 0 & 0 \\ K_v & 0 \end{bmatrix} \begin{Bmatrix} \dot{U} \\ p \end{Bmatrix} + \begin{bmatrix} K & K_v^T \\ 0 & \frac{1}{\gamma_w} K_h \end{bmatrix} \begin{Bmatrix} U \\ p \end{Bmatrix} = \begin{Bmatrix} F \\ Q \end{Bmatrix} \quad (12)$$

Eq. (12) can be solved using a dynamic procedure. The variables are the soil displacements and the excess of pore water pressure with time. One of the procedures used in this work is the application of the finite difference method with time along with Galerkin's method for theta values. This approximate quantities are referred as the external forces on soil surface  $F$ ; the induced inflow charges  $Q$ ; the excess of pore water pressure on the soil  $p$ ; the displacements of soil mass, as well as the rate of movement in terms of velocity.

$$\begin{aligned} \{F\} &= \{F_a\} + \theta \{F_b\} - \{F_a\} \\ \{Q\} &= \{Q_a\} + \theta \{Q_b\} - \{Q_a\} \\ \{p\} &= (1 - \theta) \{p_b\} + \theta \{p_a\} \\ \{U\} &= (1 - \theta) \{U_b\} + \theta \{U_a\} \\ \{\dot{U}\} &= \{U_b\} - \{U_a\} / \Delta t \end{aligned} \quad (13)$$

where:  $\{F_a\}$ ,  $\{Q_a\}$ ,  $\{p_a\}$  and  $\{U_a\}$  are the initial vectors,  $\{F_b\}$ ,  $\{Q_b\}$ ,  $\{p_b\}$  and  $\{U_b\}$  are the vectors at certain time,  $\theta$  is the value of Galerkin's parameter on the numerical solution of evolution over time,  $\Delta t$  is the increment of time that avoid numerical oscillations according to the following relationship (for triangular finite elements).

$$\Delta t \leq \frac{\alpha}{1 - \theta} \quad \alpha_{\min} = \frac{2A}{9C_v} \quad (14)$$

where:  $A$  is the area of the linear triangular finite element,  $C_v$  is the coefficient of consolidation for the soil.

A Fortran code has been developed based on the proposed algorithm along with some visualization tools. Fig. 1. shows the flow chart of the coupled model.

#### 4. NUMERICAL EXAMPLE

A rectangular slab of  $L=5.0$  m, with unitary width (plane strain condition) and a distributed surface stress  $F = -40$  kPa (the negative sign denotes downwards) on a layer of clay  $H=3.0$  m thick (see Fig. 2).

Displacements  $U_x$  and  $U_y$  are nil at the bottom and lateral boundaries of the soil. Furthermore, the clay layer is placed on a thin sand layer which allows outflow of water from the lower boundary. So, on this boundary the excess of pore water pressure is zero. In addition, water flow is not allowed on the upper boundary at the contact between the soil and the slab. Finally, water outflow is not allowed on lateral boundaries. The size of the sides of triangular elements in the mesh is 0.25 m.

During the dynamic analysis, the time step was taken as 50 days. The soil properties required for mechanical analysis are shown in Table 1. They represent medium values for a saturated clay [12,13].

Pore water pressure tend to dissipate when time increases. Table 2, shows the distribution of pore water pressure at times of 50, 450, and 900 days. Fig. 3 shows the distribution of the increment of pore water pressure 50 days after the load was applied. The initial pore water pressure (-32.29 kPa) below the slab is still close to the stress applied by the foundation (-40 kPa).

Fig. 4 shows a vertical profile of the evolution of the pore water pressure with time. It is plotted on the axis of excess in pore water pressures against depth. Notice that all values tend to zero as time increases.

**Table 1. Properties of clayey soil stratum for consolidation analysis**

Soil properties	Symbol	Magnitude
Elastic Modulus	E	20000 kPa
Poisson's ratio	$\nu$	0.35
Coefficient of permeability (x direction)	$k_x$	0.000117 m/day
Coefficient of permeability (y direction)	$k_y$	0.000117 m/day

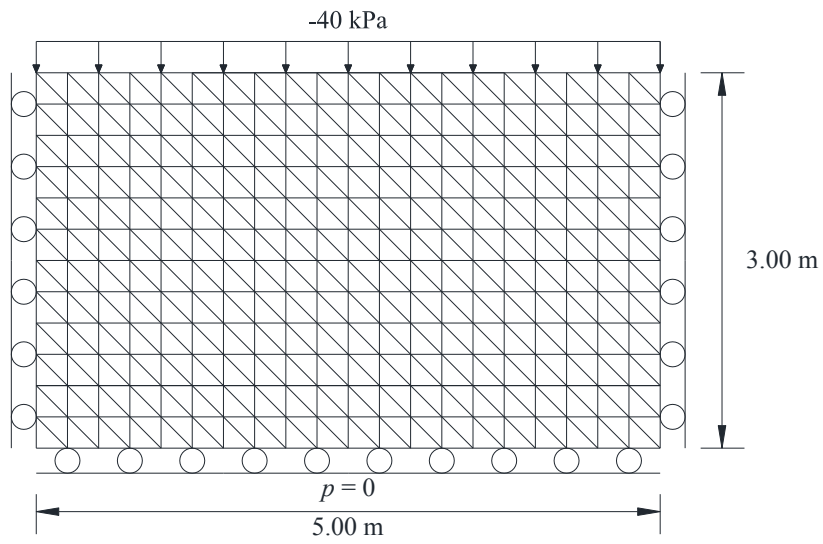


Fig. 2. Soil's domain with slab foundation applied on the surface

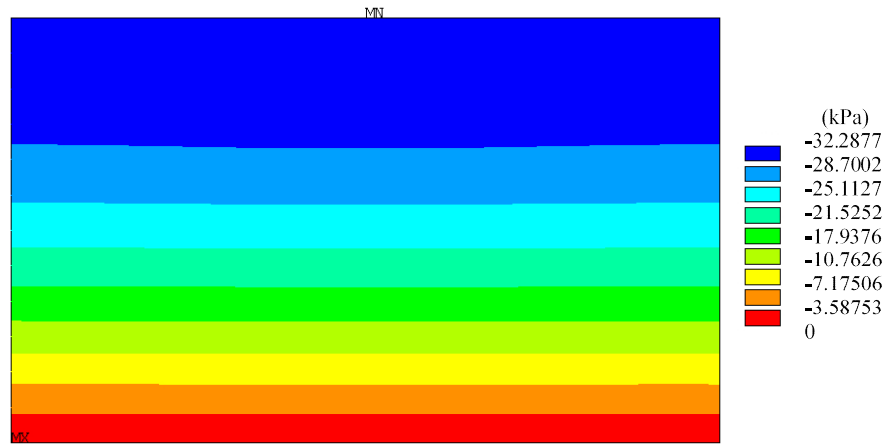
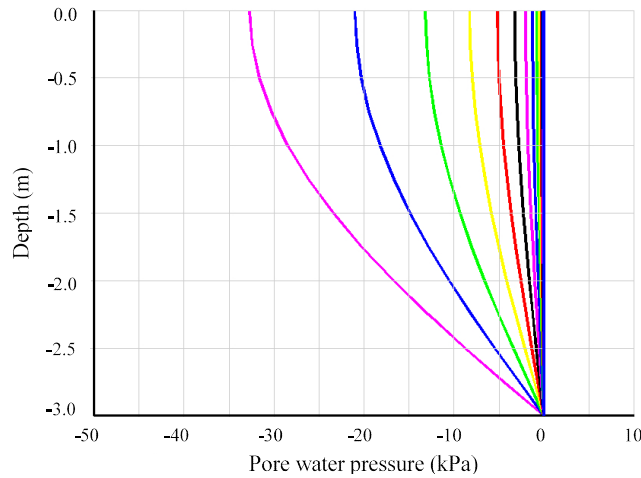


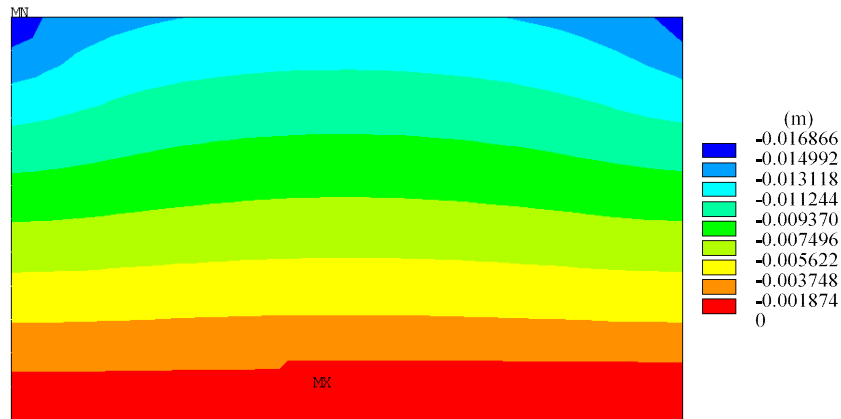
Fig. 3. Pore water pressure distribution at 50 days

Table 2. Pore water pressure distribution

Pore water pressure distribution (kPa)			
Color scale	50 days	450 days	900 days
	-32.29	$-4.63 \times 10^{-4}$	$-1.97 \times 10^{-9}$
	-28.70	$-4.12 \times 10^{-4}$	$-1.75 \times 10^{-9}$
	-25.11	$-3.60 \times 10^{-4}$	$-1.53 \times 10^{-9}$
	-21.53	$-3.09 \times 10^{-4}$	$-1.31 \times 10^{-9}$
	-17.94	$-2.57 \times 10^{-4}$	$-1.09 \times 10^{-9}$
	-14.35	$-2.06 \times 10^{-4}$	$-8.75 \times 10^{-10}$
	-10.76	$-1.54 \times 10^{-4}$	$-6.56 \times 10^{-10}$
	-7.18	$-1.03 \times 10^{-4}$	$-4.37 \times 10^{-10}$
	-3.59	$-5.15 \times 10^{-5}$	$-2.19 \times 10^{-10}$



**Fig. 4. Evolution of pore water pressure**



**Fig. 5. Distribution of vertical displacements  $U_y$**

Another main result refers to the vertical displacements. The vertical displacements due to applied loads tend to diminish with increasing time. Fig. 5 above shows the vertical displacements 50 days after the load was applied. In this figure displacements are around -0.0168 m (directed downwards) at the edge of the foundation, while at the bottom they are close to zero. The behavior of the evolution of vertical displacement is consistent with those observed in the laboratory and in the field [14]. This is evidenced in Fig. 5 and Table 3.


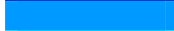







Table 3 shows the values of the displacements at 50, 450, and 900 days. Furthermore, according to Table 3, the maximum displacement observed on the surface is reached at 450 days. These displacements represent the final settlements caused by the loads transmitted

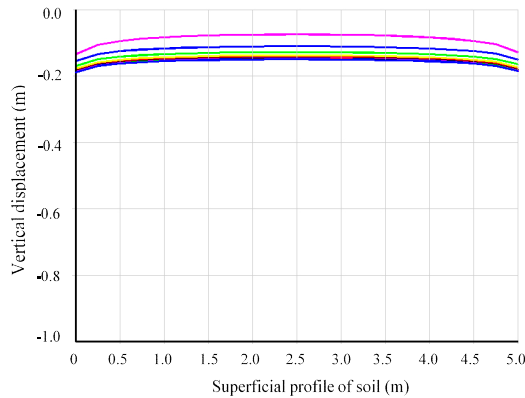
by the slab to the soil as at this time pore water pressure has almost completely dissipated. This assertion is verified through Fig. 6 which shows the evolution of displacements with time.

Another case of interest is when an isolated foundation is placed on a saturated soil as shown in Fig. 7. For the following exercise the same domain with  $L=5.0$  m was used, but only one isolated footing is placed at the center and transfers a distributed load of -40 kPa over 2.5 m. In this way those parts of the superior boundary that are not in contact with the slab, allow the water flow (1.25 m on each side of the foundation). This means that the excess in pore water pressure remains null in these zones. In addition, the lower boundary also allows water flow. The displacements are restricted in

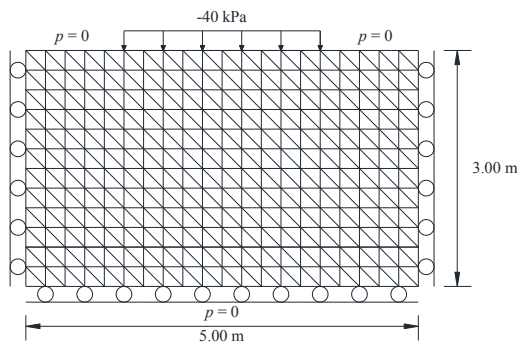
the lateral and lower boundaries (see Fig. 7). Table 4 shows the properties of the soil, the increment of time and the final time for the dynamic analysis.

**Table 3. Distribution of vertical displacements  $U_y$**

Vertical displacements $U_y$ (m)			
Color Scale	50 days	450 days	900 days
	-0.0169	-0.0189	-0.0189
	-0.0149	-0.0168	-0.0168
	-0.0131	-0.0147	-0.0147
	-0.0112	-0.0126	-0.0126
	-0.0094	-0.0105	-0.0105
	-0.0075	-0.0084	-0.0084
	-0.0056	-0.0063	-0.0063
	-0.0037	-0.0042	-0.0042
	-0.0018	-0.0021	-0.0021



**Fig. 6. Superficial profile of soil**



**Fig. 7. Soil's domain with isolated footing applied on the surface**

Fig. 8 shows the distribution of the increment of pore water pressure at a time of 30 days. Notice that the excess of pore water pressure at 30 days is still very close to the value of the applied stress on the surface. The distribution of pore water










pressures remains similar for days 450 and 870 and only the values of pore water pressures change as shown in Table 5.

Table 5 shows again that pore water pressure dissipates with time and it tends to become null at time infinity.

**Table 4. Data required for the dynamic analysis**

Data for dynamic analysis	Symbol	Magnitude
Elastic Modulus	E	20000 kPa
Poisson's ratio	$\nu$	0.35
Coefficient of permeability (x direction)	$k_x$	0.00117 m/day
Coefficient of permeability (y direction)	$k_y$	0.00117 m/day
Increment of time	$\Delta t$	30 days
Time analysis	t	900 days

**Table 5. Distribution of pore water pressure for isolated footing**

Pore water pressure distribution (kPa)			
Color Scale	30 days	450 days	870 days
	-52.38	-4.41	-0.23
	-46.56	-3.92	-0.21
	-40.74	-3.43	-0.18
	-34.92	-2.94	-0.16
	-29.10	-2.45	-0.13
	-23.28	-1.96	-0.10
	-17.46	-1.47	-0.08
	-11.64	-0.98	-0.05
	-5.82	-0.49	-0.03

Another result is the vertical profile of the pore water pressure shown in Fig. 9. This figure shows the distribution of pore water pressure with depth at 1.25 m from the left boundary. This point represents the limit of the free surface where the flow of water is allowed. Thus, the excess of pore water pressure remains null at the surface and lower boundary, while inside the domain it shows the classic evolution of double drained soils.

Moreover, Fig. 10 shows the vertical profile of the pore water pressure at 2.50 m (center of the domain). It can be observed that pore water pressure initially shows a value close to the applied stress on the surface which reduces as depth increases. In both figures, the values of pore water pressures tend to become zero at time infinity.



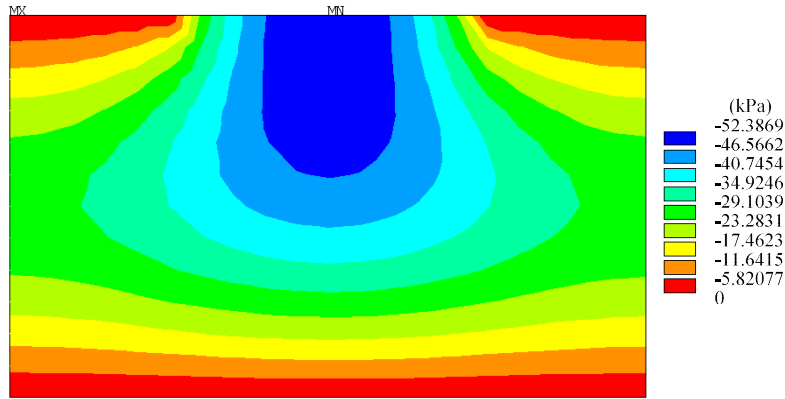


Fig. 8. Distribution of pore water pressure for isolated footing at 30 days

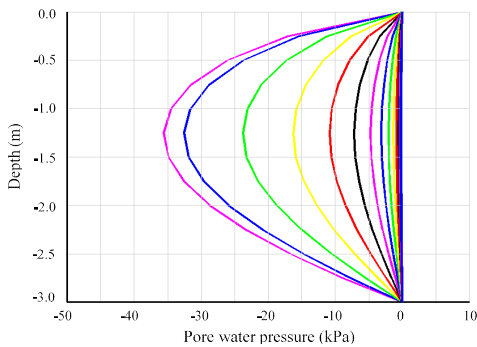


Fig. 9. Evolution of the vertical profiles of pore water pressure at 1.25 m

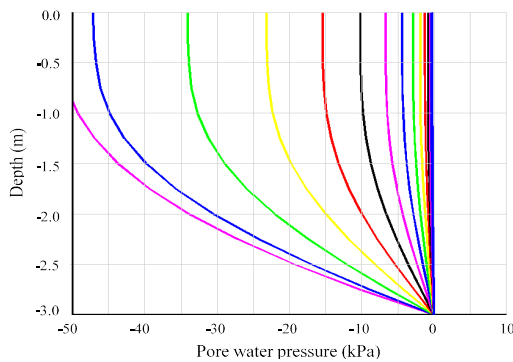


Fig. 10. Evolution of the vertical profiles of pore water pressure at 2.50 m

The model also provides diagrams of the horizontal  $U_x$  and vertical  $U_y$  displacement. They are presented in Figs. 11 and 12. Additionally, Tables 6 and 7 show the distribution of displacements  $U_x$  and  $U_y$  at different times (30, 450, and 870 days).

Table 6. Distribution of  $U_x$  displacements for isolated footing

Horizontal displacements $U_x$ (m)			
Color Scale	30 days	450 days	870 days
Dark Blue	$-1.33 \times 10^{-3}$	$-1.52 \times 10^{-3}$	$-1.51 \times 10^{-3}$
Blue	$-1.03 \times 10^{-4}$	$-1.18 \times 10^{-4}$	$-1.17 \times 10^{-4}$
Cyan	$-7.34 \times 10^{-4}$	$-8.35 \times 10^{-4}$	$-8.26 \times 10^{-4}$
Green	$-4.34 \times 10^{-4}$	$-4.91 \times 10^{-4}$	$-4.86 \times 10^{-4}$
Light Green	$-1.35 \times 10^{-4}$	$-1.48 \times 10^{-4}$	$-1.46 \times 10^{-4}$
Yellow	$1.65 \times 10^{-4}$	$1.96 \times 10^{-4}$	$1.95 \times 10^{-4}$
Orange	$4.64 \times 10^{-4}$	$5.40 \times 10^{-4}$	$5.35 \times 10^{-4}$
Red-Orange	$7.64 \times 10^{-4}$	$8.83 \times 10^{-4}$	$8.75 \times 10^{-4}$
Red	$1.06 \times 10^{-4}$	$1.23 \times 10^{-4}$	$1.22 \times 10^{-4}$

In Fig. 11 and Table 6 a characteristic phenomenon of symmetry due to loads applied at the central zone is observed. From the center line to the left, values have a negative sign. This is due to the direction in which they occur, as in the coordinate system, the y-axis is located at the center line. In contrast, the displacements on the right side from the center line are positive.

Fig. 12 and Table 7 show the evolution of the vertical displacements  $U_y$ . Furthermore, through this figure displacements are about -0.0069 m on the edge of the foundation, while near the bottom they are close to zero. Here, the negative sign indicates the direction in which the displacements evolve. Vertical displacements are produced by the load applied by the slab. Notice that displacements show a symmetrical diagram. They are also appropriate and consistent with the results reported by Magaña and Romo [5], Bentler [6], Manzolillo et al. [8], Di-Rado et al. [9] and Krishnamoorthy [10].

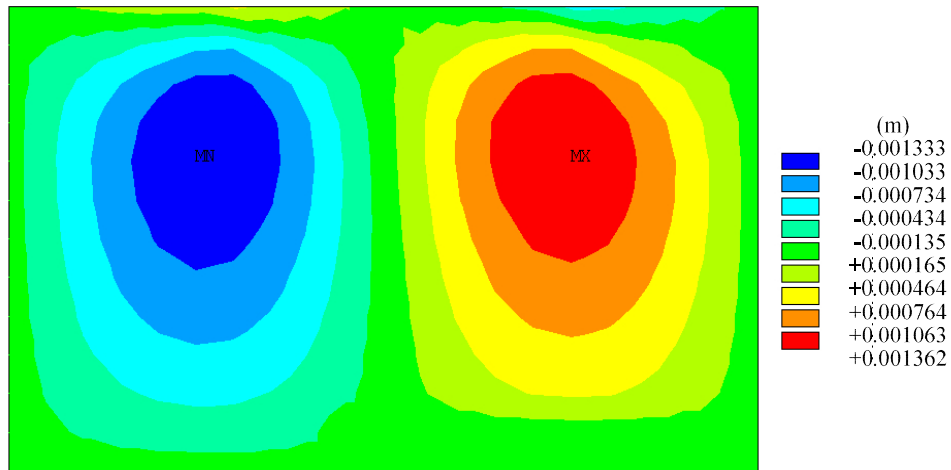


Fig. 11. Horizontal displacements  $U_x$  for isolated footing

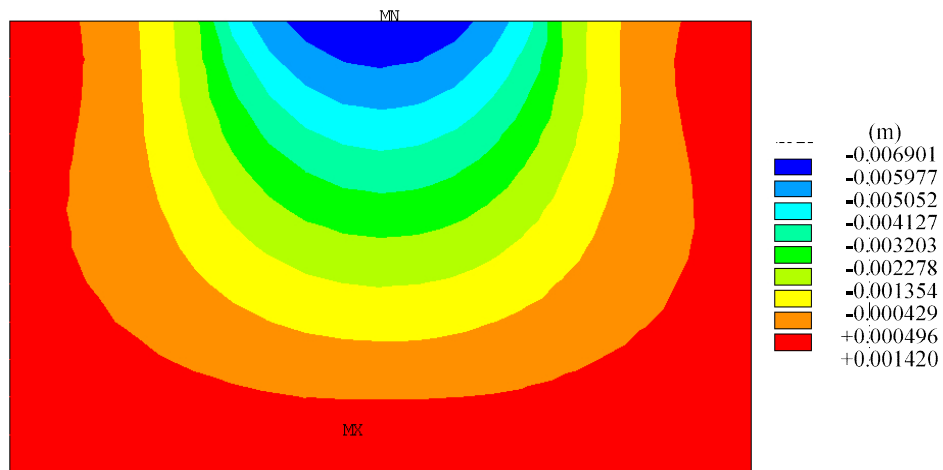


Fig. 12. Vertical displacements  $U_y$  for isolated footing

Table 7.  $U_y$  displacements for isolated footing

Vertical displacements $U_y$ (m)			
Color Scale	30 days	450 days	870 days
Dark Blue	$-6.90 \times 10^{-3}$	$-1.30 \times 10^{-2}$	$-1.30 \times 10^{-2}$
Blue	$-5.97 \times 10^{-3}$	$-1.16 \times 10^{-2}$	$-1.16 \times 10^{-2}$
Cyan	$-5.05 \times 10^{-3}$	$-1.10 \times 10^{-2}$	$-1.10 \times 10^{-2}$
Light Green	$-4.13 \times 10^{-3}$	$-8.68 \times 10^{-3}$	$-8.68 \times 10^{-3}$
Green	$-3.20 \times 10^{-3}$	$-7.23 \times 10^{-3}$	$-7.23 \times 10^{-3}$
Yellow-Green	$-2.28 \times 10^{-3}$	$-5.79 \times 10^{-3}$	$-5.79 \times 10^{-3}$
Yellow	$-1.35 \times 10^{-3}$	$-4.34 \times 10^{-3}$	$-4.34 \times 10^{-3}$
Orange	$-4.29 \times 10^{-4}$	$-2.89 \times 10^{-3}$	$-2.89 \times 10^{-3}$
Red	$+4.96 \times 10^{-4}$	$+1.45 \times 10^{-3}$	$+1.45 \times 10^{-3}$

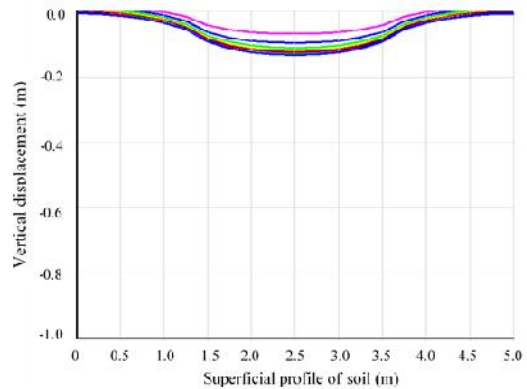


Fig. 13. Superficial profile of soil for isolated footing

Fig. 13 shows the surface profile of vertical displacements. Again, notice that they are negative (directed downwards) and the maximum value (-0.0130 m) occurs at the center of the domain, i.e., at the center of the slab. In addition, in the free surface areas (where stresses are not applied) they show positive values. This means that, in these areas, the soil moves upwards while the slab sinks.

## 5. CONCLUSIONS

The coupled model algorithm presented herein, shows appropriate results and uses few basic soil parameters. It is flexible, allowing infinite combinations of load, displacements and pore water pressure at the boundaries. Therefore it can reproduce different field or laboratory conditions. It may consider water intake or outtake through the flow vector  $\{Q\}$ . The evolution of pore water pressure as well as horizontal and vertical displacements can be observed. Furthermore, the results show an appropriate behavior of the phenomenon of consolidation of saturated soils when compared to other models and experimental results.

Another advantage of this model is that it can be extended for the case of unsaturated soils. This is possible only by replacing the effective stress equation of saturated soils to that of unsaturated materials and by introducing a model for the retention curve during wetting-drying cycles. In such a case the effective stress parameter  $\chi$  and the hydraulic permeability of the soil can be determined for any value of suction. In the future, efforts will be aimed towards unsaturated consolidation through this model.

## ACKNOWLEDGEMENT

The authors would like to thank to the Consejo Nacional de Ciencia y Tecnología (CONACYT) and the Universidad Autónoma de Querétaro.

## COMPETING INTERESTS

Authors have declared that no competing interests exist.

## REFERENCES

- Inoue N, Romanel C, Roehl D, Análisis por el método de los elementos finitos de la consolidación de suelos no saturados, 4to Congreso Internacional, 2do Congreso Nacional de Métodos Numéricos en Ingeniería y Ciencias Aplicadas. México; 2007.
- Ali MM, Identifying and analyzing problematic soils. *Geotech. Geol. Eng.* 2011;29:343-350.
- Al-Shamrani MA, Dhownian AW, Experimental study of lateral restraint effects on the potential of expansive soils. *Engineering Geology*, 2003;69:63-81.
- Jones LD, Jefferson I, Expansive soils. In: Burland, J. *Institution of Civil Engineers (ICE) manual of geotechnical engineering*. ed. London, UK.: ICE Publishing; 2012.
- Magaña R, Romo MP, Modelo numérico para estudiar el movimiento de agua en suelos no saturados. *Instituto de Ingeniería, Universidad Nacional Autónoma de México*. 1980;1-23.
- Bentler DJ, Coupled consolidation, Finite element analysis of deep excavations. 1998;83-102.
- Wong TT, Fredlund DG, Krahn J, A numerical study of coupled consolidation in unsaturated soils. *Canadian Geotechnical Journal*. 1998;35:926-937.
- Manzolillo JE, Di-Rado HA, Awruch AM, Simulación numérica del comportamiento de suelos saturados bajo cargas de fundaciones. *Comunicaciones Científicas y Tecnológicas, Universidad Nacional del Nordeste*; 2000.
- Di-Rado HA, Beneyto PA, Mroginski JL, Manzolillo JE, Awruch AM, Análisis tridimensional de la consolidación de suelos saturados utilizando el MEF, *Mecánica Computacional*. 2004;23:607-617.
- Krishnamoorthy MS, Consolidation analysis using finite element method. *The 12th International Conference of International Association for Computer Methods and Advances in Geomechanics (IACMAG)*. 2008;1157-1161.
- Tsiampousi A, Smith P, Potts D, Coupled consolidation in unsaturated soils: From a conceptual model to applications in boundary value problems. *Computers and Geotechnics*. In press; 2016. Available:<http://dx.doi.org/10.1016/j.compgeo.2016.10.008>
- Gurtin ME, *An introduction to continuum mechanics, Mathematics in Sciences and Engineering*. Academic Press Elsevier; 2003.

13. Pérez-Rea ML, Predicción de propiedades mecánicas y reológicas de suelos usando teoría de percolación. Ph. D. thesis. Instituto Tecnológico y de Estudios Superiores de Monterrey. Estado de México, México; 2005.
14. Vásquez-Nogal I, Impacto en la conductividad hidráulica en la modificación con cal en suelos expansivos. M. Sc. Thesis, Universidad Autónoma de Querétaro. Querétaro, México; 2016.

---

© 2016 Rangel et al.; This is an Open Access article distributed under the terms of the Creative Commons Attribution License (<http://creativecommons.org/licenses/by/4.0>), which permits unrestricted use, distribution, and reproduction in any medium, provided the original work is properly cited.

*Peer-review history:*  
*The peer review history for this paper can be accessed here:*  
<http://sciencedomain.org/review-history/17112>